AD-A214 963

REPORT DOCUMENTATION PAGE

Form Approved
OMB No. 0704-0188

1. AGENCY USE ONLY (Leave blank)	2. REPORT DATE	3. REPORT TYPE AND DATES COVERED
	Dec 81	Final (1 JAN 82 - 31 Dec 81

4. TITLE AND SUBTITLE

HIGH-RESOLUTION ASTROPHYSICAL OBSERVATIONS USING SPECKLE IMAGING

5. FUNDING NUMBERS

61102F
2311/A1

6. AUTHOR(S)

Robert W. Noyes
Peter Nisenson
Robert V. Stachnik

7. PERFORMING ORGANIZATION NAME(S) AND ADDRESS(ES)

Smithsonian Institution
Astrophysical Observatory
Cambridge, MA, 02138

AFOSR-TR-

8. PERFORMING ORGANIZATION REPORT NUMBER

9. SPONSORING/MONITORING AGENCY NAME(S) AND ADDRESS(ES)

AFOSR
BLDG 410
BAFB DC 20332-6448

10. SPONSORING/MONITORING AGENCY REPORT NUMBER

AFOSR-81-0055

11. SUPPLEMENTARY NOTES

12a. DISTRIBUTION/AVAILABILITY STATEMENT

Approved for public release;
distribution unlimited.

12b. DISTRIBUTION CODE

13. ABSTRACT (Maximum 200 words)

The reconstruction of complex solar surface features to a factor of ~~four~~ ten finer than could normally be studied under prevailing seeing conditions has been demonstrated Previously, sucessful examples of speckle image reconstruction were limited to uncomplicated objects showing very high contrast structure. The ability to retrieve complex and low contrast image detail is a result of recognizing the need for high quality sensors capable of recording subtle intensity modulations in the data frames.

14. SUBJECT TERMS	15. NUMBER OF PAGES
	18
	16. PRICE CODE

17. SECURITY CLASSIFICATION OF REPORT	18. SECURITY CLASSIFICATION OF THIS PAGE	19. SECURITY CLASSIFICATION OF ABSTRACT	20. LIMITATION OF ABSTRACT
unclassified	unclassified		

HIGH-RESOLUTION ASTROPHYSICAL OBSERVATIONS

USING SPECKLE IMAGING

Contract AFOSR-81-0055

Annual Report

For the period 1 January 1981 through December 31 1981

Robert W. Noyes Principal Investigator
Peter Nisenson Coinvestigator
Robert V. Stachnik Coinvestigator

Prepared for

Air Force Office of Scientific Research
Bolling Air Force Base
Washington, D.C. 20332

Smithsonian Institution
Astrophysical Observatory
Cambridge, Massachusetts 02138

The Smithsonian Astrophysical Observatory
and the Harvard College Observatory
are members of the
Center for Astrophysics.

The Scientific Program Officer for this contract is
Dr. Henry Radoski, AFOSR, Bldg. 410, Bolling AFB, Washington, DC 20332

I. INTRODUCTION

Under the present Air Force Office of Scientific Research grant, we have demonstrated reconstruction of complex solar surface features to a factor of ten finer than could normally be studied under prevailing seeing conditions. Previously, successful examples of speckle image reconstruction were limited to uncomplicated objects showing very high contrast structure. Our ability to retrieve complex and low contrast image detail is a result of recognizing the need for high quality sensors capable of recording subtle intensity modulations in the data frames. We have learned that this is a crucial requirement.

In the past, computer simulations of the speckle process have proven far more impressive than have laboratory simulations or on-telescope tests. The latter have not provided very accurate representations of the input source except for simple targets. We believe that this discrepancy was the result of sensor limitations, in particular, inadequate dynamic range and linearity. Subsequent tests have borne out this suspicion.

We have addressed the problem of accurate image recording in two ways. In the high light level regime, appropriate to solar surface imaging, we have moved to use of solid state image sensors (CCD's and CID's). These devices have more than an order of magnitude greater dynamic range than the video detectors used in earlier experiments. The effect of improved detector response on our reconstructions has been dramatic. We are now in the process of acquiring our own CCD image recording system, optimized to the requirements of speckle data collection, which will have a data rate 15 times that used in our first CCD experiments.

At lower light levels, the central problem has been accurate correction for the effects of photon noise. The solution here is a photon counting camera. Such a device has a dynamic range set by digital, rather than analog, storage considerations and the demanding sensor requirements discussed above can actually be

more easily met at low light levels than high. A very promising photon counting camera of innovative design is under development for use in the speckle project in collaboration with Dr. Costas Papaliolios, also of the Center for Astrophysics. The new camera has already undergone preliminary testing. Finally, we have recently completed an extensive simulation program to examine the effects of sensor limitations on image recovery, and have undertaken a series of experiments to study the structure of supergiant chromospheres.

II. TECHNICAL BACKGROUND

Speckle imaging shares many of the characteristics of the more widely used speckle interferometry; the difference is in the processing algorithm, which produces true images instead of spatial autocorrelations. In both processes, a series of images is recorded with exposure times short compared to the fastest motions of atmospheric turbulence (~ 10 ms). If these images are recorded in a narrow spectral bandwidth, and if the reconstructed area is restricted to a few arcseconds (this is the "isoplanatic patch" requirement set by upper level turbulence strength), then the distortion of the incoming wavefront by the atmosphere can be nearly eliminated by an averaging procedure.

The speckle image processing algorithms are based on an approach suggested by Knox and Thompson (1974) and developed and demonstrated for two-dimensional extended, continuous tone objects by Nisenson *et al.* (1980).

Briefly, the algorithm requires many individual images to be recorded. The individual images are then fourier-transformed and the transform amplitudes and point-to-point phase differences are separately averaged. This procedure preserves the diffraction-limited image information encoded in individual short exposures and, after recovering the fourier transform phases from the averaged phase differences, and transformation back to image space, a high resolution reconstructed image can be obtained. A more detailed description of the process follows.

In the imaging process, the phase in the fourier transform of each frame is encoded in the form of point-to-point phase differences. This is performed in two dimensions by calculating the shifted complex product of the transform. The results for each frame are summed, yielding averaged quantities $\langle A_u(u,v)\rangle$ and $\langle A_v(u,v)\rangle$ ($\langle\rangle$ indicates an ensemble average) in the form

$$\begin{aligned} \langle A_u(u,v)\rangle &= \langle I(u,v)I^*(u+\Delta u,v)\rangle \\ \langle A_{v(u,v)}\rangle &= \langle I(u,v)I^*(u,v+\Delta v)\rangle \end{aligned} \tag{1}$$

where I(u,v) is the image fourier transform and the two averages encode the phase in the u and v directions, respectively. The shifts, δu and δv, must be small compared to the correlation length in the object transform.

Each of the components in Eq. (1) can be expanded in the form

$$\begin{aligned} \langle A(u,v)\rangle \approx= |O(u,v)|^2 \exp\{i[\phi(u,v) - \phi(u+\Delta u,v)]\} \\ x\langle |T(u,v)|^2 \exp\{i[\psi(u,v) - \psi(u+\Delta u,v)]\}\rangle \end{aligned} \tag{2}$$

where O(u,v) is the object fourier transform, T(u,v) is the atmospheric transfer function, and $\phi(u,v)$ and $\psi(u,v)$ are the phase in the object transform and the atmospheric transfer function, respectively.

The transfer function term in Eq. (2) has an expected value whose phase approaches zero (since the atmospheric phase fluctuations are a stochastic, zero mean process) and whose amplitude approaches the diffraction limited transfer function usually obtained in conventional speckle interferometry. For reconstruction, the relative phase at any point in the transform is calculated by summing the phase differences between that point and an arbitrary reference point. An iterative relaxation algorithm is applied, yielding a least squares estimate of the phases. Finally, the output image is obtained by fourier inversion of the resulting phase and amplitude distribution.

III. SOLAR RESULTS

The data described in these experiments consisted of direct images of small

patches of the solar surface recorded with a liquid nitrogen-cooled General Electric charge injection device (C.I.D.). The data were obtained at the Kitt Peak 1.5-meter McMath telescope 16-18 July, 1981, and were recorded as 120 x 248-element 12-bit digital images. The seeing in all processed data sets was 2 arcsec, or better. A 10 nm bandpass, 410 nm central wavelength interference filter was used with a shutter having an exposure time of no more than a few milliseconds. The narrow bandwidth eliminated the need for atmospheric dispersion compensation. A practical restriction on the number of images recorded in a data-taking sequence was the fact that images had first to be read onto a disk before being copied to tape. This limited us to a maximum of 60 frames before dumping to tape. Furthermore, device readout restrictions necessitated an image recording cycle time of one image every 1.7 seconds. Consequently, recording a 60-frame data set took slightly over 100 seconds.

The image recording system included two optical paths. In one, the image was relayed through a shutter and a 2 x 2 magnifying lens onto the C.I.D. sensor. In the second, a folding mirror transmitted an unmagnified image to a T.V. camera. Except for the very brief intervals of C.I.D. exposure, the second optical path allowed continuous field finding and guiding. The output of the video camera was recorded to provide a record of the low magnification field. Because of the magnification difference for the two optical paths and the differing areas of the photosensitive surface, the scale in the low magnification field was about one quarter that of the high magnification field.

Figure 1 shows 9 of the 46 frames used to produce a reconstruction of a single pore approximately 4 arcseconds across. The field is 5x6 arcseconds in size. Seven of the nine frames are among those rated as containing the largest amount of high frequency detail during the image preview procedure. The two top frames in the right column were noted as being "poor" and "fair," respectively. Although

very fine structure is evidently present in the raw images, it differs in detail from frame to frame, suggesting that this is "speckle," not true image detail.

Figure 2 shows the result of speckle processing two 23-frame subsets of the data. Reconstruction C is produced from frames 1, 3, 5, etc., while D is produced from frames 2, 4, 6, etc. Both a single frame (A) and a 46-frame direct sum (B) are also included. There are substantial similarities between the two reconstructions, but also some differences at the finer scales.

The total number of available frames is too small to insure complete convergence at the highest spatial frequencies and the 23-frame subsets are even more likely to suffer from inadequate convergence. 100 to 200 frames are usually required at high light levels. Much of the difference between subsets is probably due to the convergence problem, although differences in normalization also affect the reconstructions differently. Some variation between reconstructions may also arise from differences in details of the image wander with respect to the border. The basic "C"-shaped structure of the reconstructed pore and the presence of three darker, and, presumably, cooler areas on the "C" seems to replicate in the two subset reconstructions.

Figure 3 is a reconstruction of penumbral structure associated with a somewhat larger spot. At top left (A) is the large-scale (20 x 20 arcsecond) field showing the subarea we chose to process. At top right (B) is the small (5 x 6 arcsecond) field, obtained by direct summation of the images. At lower left (C), is a power spectrum for the processed area. The elongated feature in the power spectrum is evidence of considerable anisotropy in the distribution of high frequency image structure. The orientation is unsurprising since it implies the presence of linear feature radial to the spot penumbra. What is interesting is the extent, in frequency space, of the elongated feature. Power spectrum analysis (speckle interferometry) is relatively simple and well understood, and we find, for

these data, that considerable power is present out to a spatial frequency corresponding to 0.1 arcsecond. The reconstruction, D, shows the corresponding image structure. The 0.1 arcsecond detail is at a scale much finer than that usually associated with spot penumbrae, approaching the diffraction limit, .055 arcsec (at λ_c = 4100Å), of the McMath telescope. The data are, in fact, somewhat undersampled with respect to the Nyquist criterion and the tenth arcsecond cut-off may well be due only to the sampling limitation.

Figure 4 shows power spectra and reconstructions at three adjacent locations near the lower right quadrant of the small spot visible in the low magnification image at the top of the figure. Data set B is the same as that in Figure 3. Data sets A and C are, respectively, above and below it. The fact that the high frequency structure depicted in both the power spectra and recovered images rotates in a way suggesting that the fine filamentary structure is oriented radially to the spot are consistent with one's expectations for penumbral detail.

Finally, Figure 5 shows the recovered image for a pair of small pores immersed in the penumbra of a larger spot complex. At top left (A) is the low magnification image and at top right (B) is the high magnification field. At bottom right (D) is the recovered image. The very best individual input frames also show evidence that the striations penetrate to the center of the pore, as they clearly do in the reconstruction. The power spectrum (C) is consistent with linearly-organized structures having significant power on a spatial scale of 0.2 arcseconds. The reconstruction may offer evidence that the magnetic field structure at the center of a pore can be dominated by the field associated with the the penumbra of a large nearby spot.

Finally, other reconstructions (not shown) demonstrate that not all broadband features show complex internal structure. At least one pore reconstructed to a rather uniform feature only a bit smaller in size than that seen in the best individual

images.

To summarize the results of this single observing run:

- A reconstruction of a pore approximately four arcseconds in size, shows evidence for multiple (3) subareas darker, and presumably cooler, than the rest of the pore. The pore is also brightened toward the center.

- The recovered image of a small patch of penumbra shows very fine 0.1 arcsecond filamentary detail embedded in the coarser and more familiar radial penumbral structure. Detection of 0.1 arcsecond structure implies resolution near the telescope diffraction limit.

- The recovered image of a pair of pores embedded in the penumbra of a nearby large spot suggests that their internal morphology is determined as much by the surrounding penumbra as by their own magnetic fields.

- Not all features show complex internal structure.

IV. STUDIES OF SUPERGIANT CHROMOSPHERES

A major experiment conducted with the intensified ISIT videocamera involved attempts at detecting chromospheric emission, at Hα, around supergiant stars. This work was done in collaboration with Dr. Leo Goldberg of KPNO.

Speckle observations of several supergiant stars, obtained at the KPNO 4-meter telescope, were prompted by the consideration that these objects show Hα emission, are angularly large, and that models indicate, (in contrast to the case of the Sun) the likelihood of chromospheric radii significantly different from the photospheric radii. The observations involved recording speckle data for both supergiants and reference stars through a narrow band (2.5Å) filter which could be tuned alternately on or off the line. Comparison of on-line autocorrelations with off-line autocorrelations, as calibrated by on-versus off-line observations of hot, angularly small reference stars, can reveal the presence of circumstellar emission structure.

A fairly extensive data set was recorded for a number of different supergiants, along with data on hotter stars, which should not have extended chromospheres, to use for reference stars.

Processing of the narrowband data has not yielded positive results. The extended chromospheres are expected to yield only a fairly weak signal, and the signal-to-noise of data recorded with the ISIT video system appears to be insufficient. This is due to the fact that the intensified ISIT can operate only in an analog photon sensing mode. Since the device is not a true photon counter, accurate photon noise compensation, required for very narrow band work, was not possible. Experiences of this sort have underscored the need for a reliable, high data rate photon counting camera to allow speckle image processing to achieve its full scientific potential.

An experiment by Dr. Francois Roddier of Nice Observatory, using a coherence interferometer, indicates that significant scattering, presumably by dust, may occur in continuum radiation as well as in lines. We are now studying data sets obtained with larger passband filters, for which photon noise bias influences are less severe, for evidence of such an effect. Preliminary inspection of the reconstructions suggest a possible detection of circumstellar continuum scattering for g Herculis, an M III star.

V. NUMERICAL EXPERIMENTS

A series of analytic experiments were carried out in order to determine the effects of various recording and at associated parameters on the speckle image reconstruction process. A series of images of an unresolved bright star, Alpha Lyrae, recorded with the ISIT video speckle system at the KPNO 4-meter telescope, were convolved with a computer generated test pattern: the Greek letter Γ plus an unresolved point. 200 separate frames were generated this way and they were used to test the effects of photon noise, limited detector dynamic range, and other

parameter . n the reconstruction process. Another 200 frames of data, recorded a shor- .nile after the data used for the convolutions, was integrated and used as a reference source for tranfer function reweighting.

Figure 6a-f demonstrate the effects of photon noise on the reconstruction process. Figure 6a shows a typical input frame. Photon noise has been introduced into the data by replacing the intensity at each pixel with a Poisson-distributed random number having a mean equal to the intensity. In the data set shown here, the main value was 300 photons per object pixel, which corresponds to the detected flux level from an object having approximately a brightness of 11th magnitude per resel for a 250Å bandpass at the 4-meter telescope with a 20% Q.E. detector. Figure 6b shows the image for a 200-frame direct sum of the data sets. Figure 6c, 6d and 6e show the results of correcting the data for the bias term introduced in the amplitudes and phases by the photon noise. The bias should be proportional to the expected number of photons in the average, $\bar{N}$. Figure 6c shows the reconstruction with no bias correction. In Figure 6d, the bias correction scale factor is set to $\bar{N}/2$ while in 1e the scale factor is $\bar{N}$. Clearly, exact setting for the bias correction is critically important for obtaining accurate reconstructions. Figure 6f show the reconstruction from a 200 frame data set with a 15 times higher flux level, approximately equal to 8th magnitude per resel. It is interesting to compare the results in 6e to 6f. Though 6e is substantially fainter, the result is only a somewhat noisier and less sharp image, with no artifacts introduced into the reconstruction. At the 6e light level, 2000 frames are expected to be required for a diffraction-limited recovery, while at the 6f light level less than 100 frames are required for photon noise convergence (however, 100 frames may not be adequate to average out all atmospheric effects).

Tests have been carried out with data corresponding to a factor of 100 fainter than in Figure 6a-6e. The 200-frame reconstructions were much less sharp and

noisier, but the images were recognizable and artifact free.

We have used the same approach to test camera limitations. Figure 7a-7d show an example of the tests of the effect of camera dynamic range on the reconstruction process. In this case the data was adjusted to have a limited number of gray levels, testing a camera with limited dynamic range. One would predict that the number of gray levels required for accurate image recovery should be several times greater than the number of resels in the object (if the object is smaller than the seeing disk). In this case, the Γ had 350 resels, so close to 1000 gray levels should be needed. Figure 7a-7d show results for 20, 100, 1000 and no quantization. Clearly 20 gray levels is far too few. 100 gray levels is approximately the range available in our ISIT video system; still too few for better than 5 to 10% accuracy in the reconstruction intensity. For 1000 gray level one obtains a very accurate reconstruction, though there is still some degradation from the "no quantization" case shown in 7d.

These results emphasize the requirement for a linear wide dynamic range camera for recording speckle data if one wishes to obtain accurate reconstructions. A carefully flat-fielded CCD camera meets these requirements for bright objects while a photon counting camera would have an unlimited dynamic range for faint objects.

The experimental procedure has proven very useful in evaluating the experimental requirements of the process. Some of the other parameters under investigation utilizing this technique are the effects of a fixed pattern background introduced by the detector and the influence of the frame borders on the reconstruction of data extending outside the edge of the field.

VI. SUMMARY

In the past year we have pursued most actively a program of solar surface image reconstruction, using data recorded with a solid-state array detector. These experiments have been extremely successful, resulting in image reconstructions

showing a factor of 10 improvement in resolution. An important finding is that the image reconstruction programs now in place can produce useful reconstructions provided that the processed data are accurately recorded and have a high signal-to-noise ratio.

We have carried out, as well, a series of highly realistic numerical experiments which enabled us to better understand the varied effects of sensor limitations. Finally, we have carried out a series of broad and narrow band speckle observations of cool supergiant stars in an effort to detect extended chromospheric structure or the presence of other circumstellar material. This latter work is still in progress.

Fig. 1

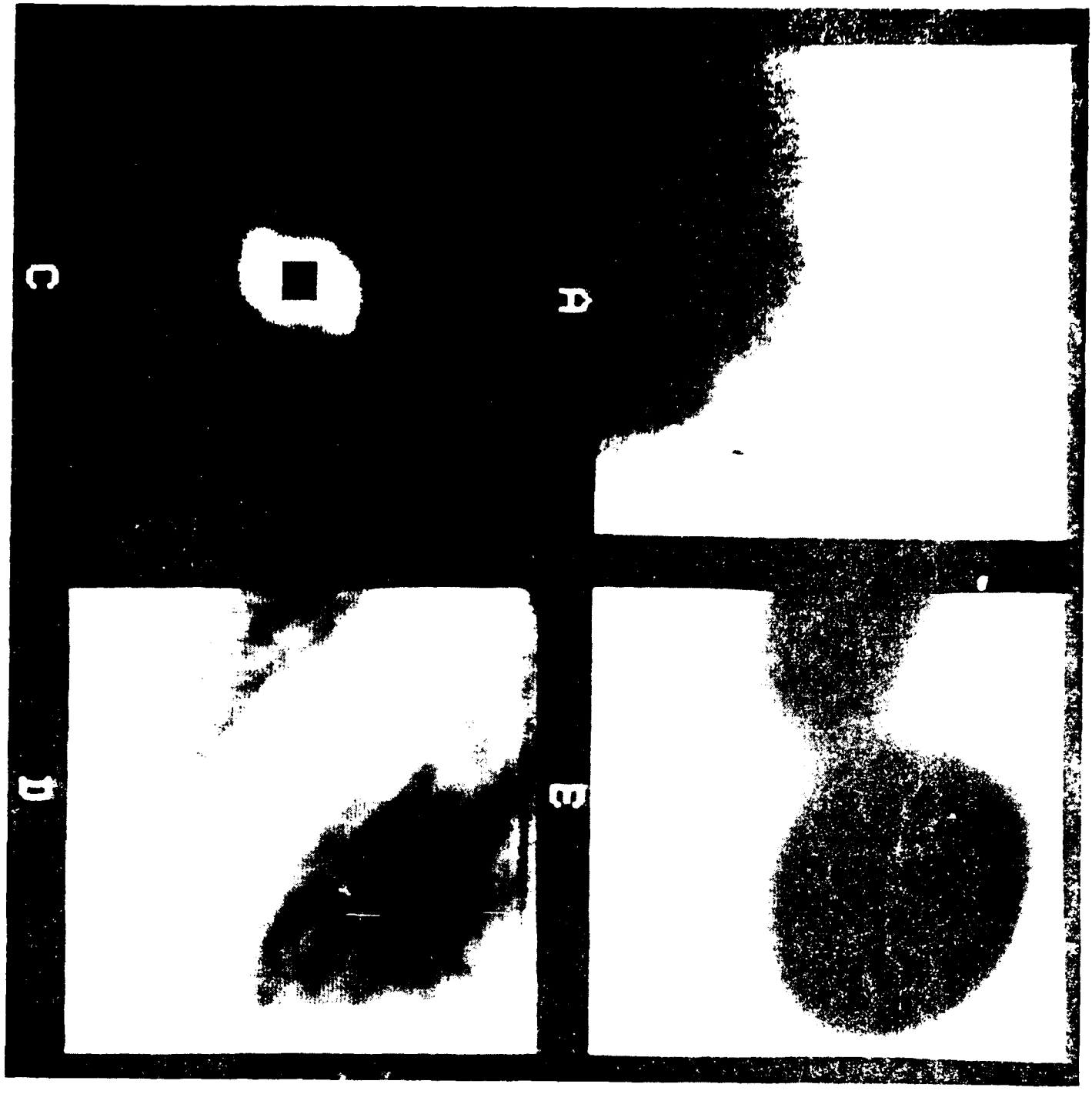

Fig. 2

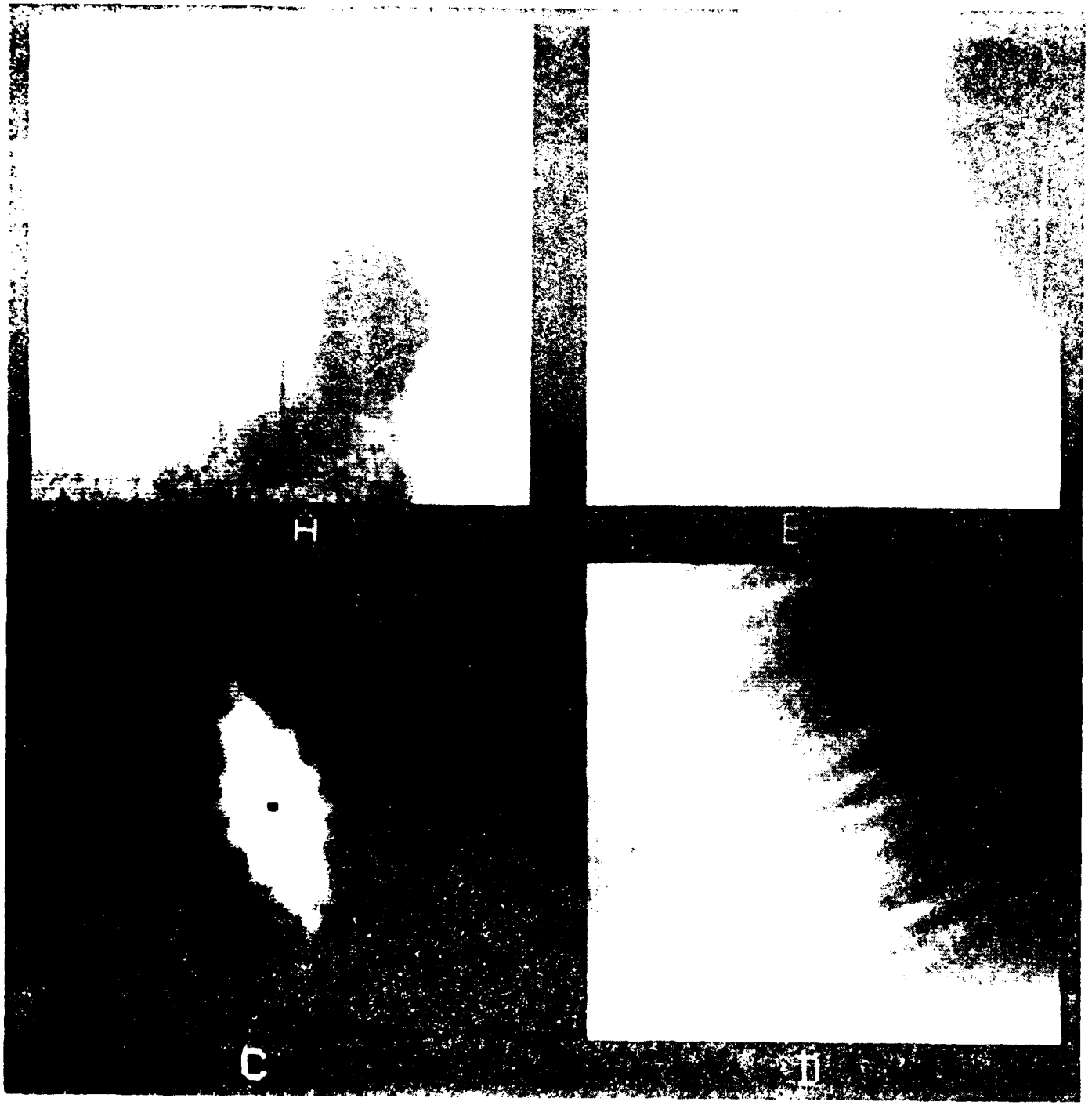
H
E
C
D

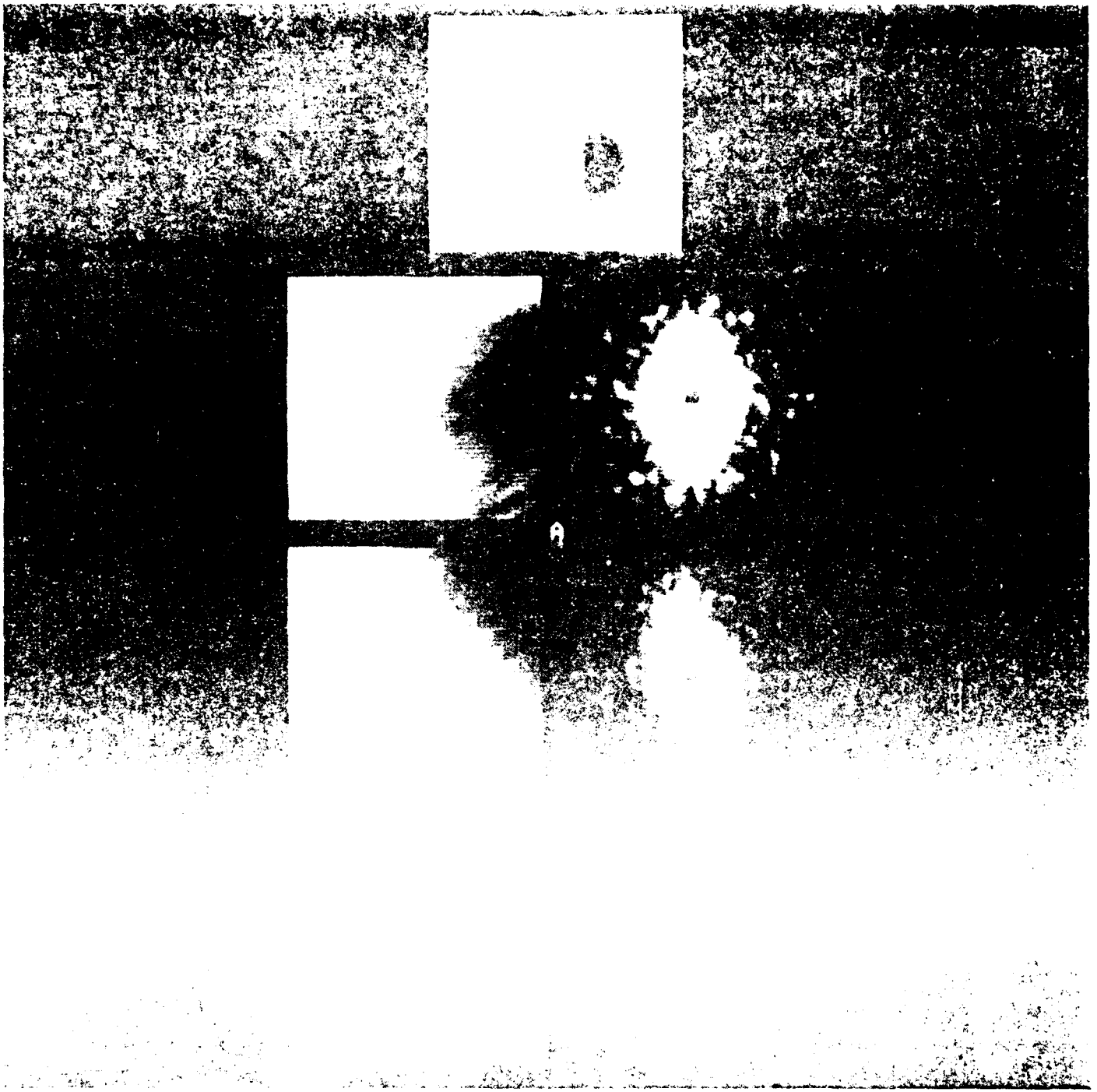

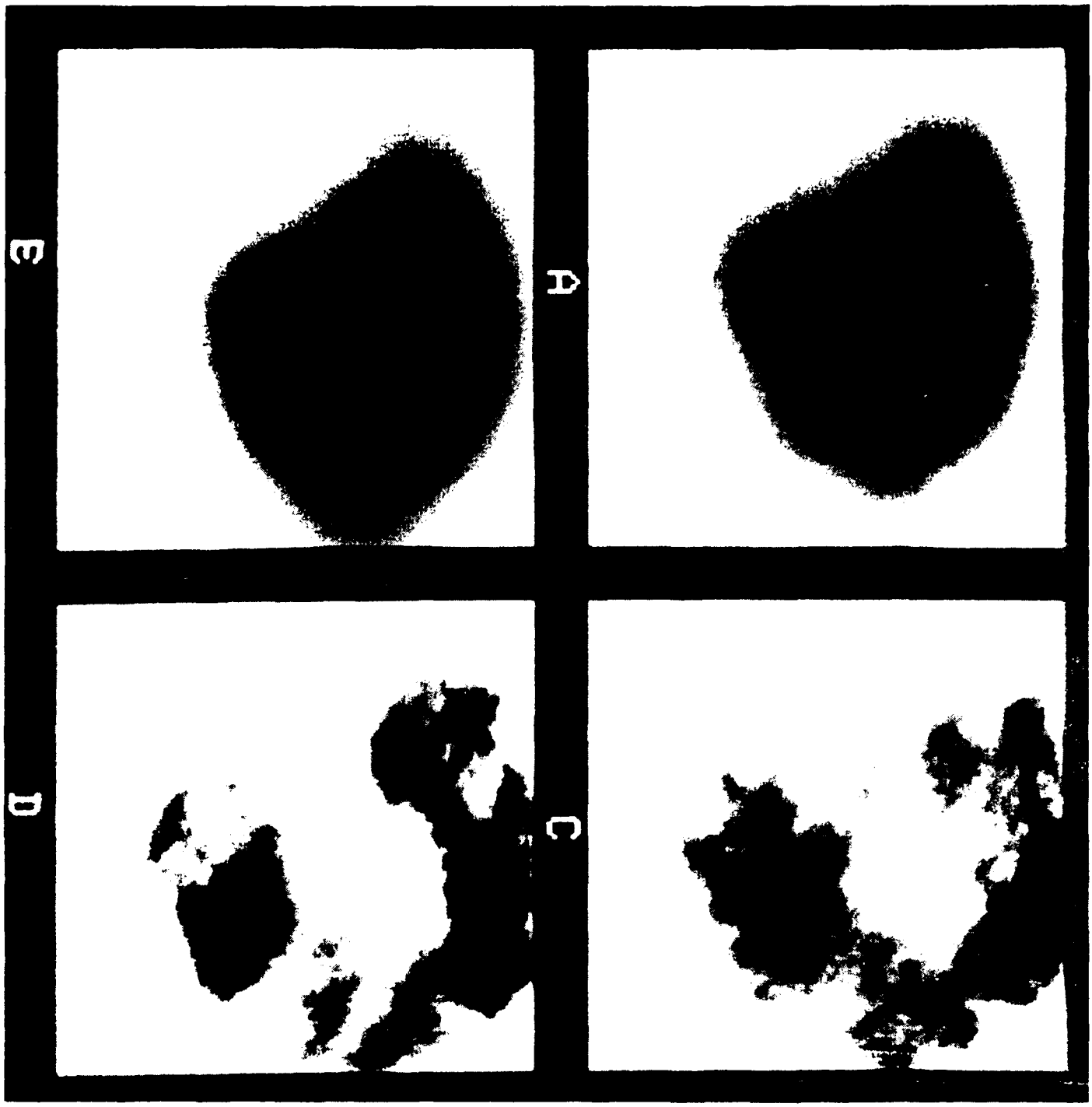

Fig. 5

Fig. 6

Fig. 7